A Drive-by Bridge Damage Localisation Method with an Instrumented Vehicle

Xuzhao Lu[1], Limin Sun[1], Chul-Woo Kim[2](✉), Kai-Chun Chang[2], and Zhuoran Han[2]

[1] Tongji University, Shanghai 200082, China
{luxuzhao_1992,lmsun}@tongji.edu.cn
[2] Kyoto University, Kyoto 615-8540, Japan
{kim.chulwoo.5u,chang.kaichun.4z}@kyoto-u.ac.jp,
han.zhuoran.78r@st.kyoto-u.ac.jp

Abstract. Damage localisation is an important issue in bridge health monitoring. It helps to develop further maintenance strategies. For long-term monitoring, the traditional method is to install sensors on the bridge of interest. Then, by checking the vibration frequencies, mode shapes or some other indices, the damage location was expected to be identified. However, for short and medium span bridges on urban highway systems, the traditional method requires a large number of sensors, which is time consuming and labour intensive. This study aims to discuss the feasibility of a novel damage localisation method based on the characteristics of the Vehicle-Bridge Interaction (VBI) system. A drive-by method is proposed to check the damage location with a drive-by instrumented moving vehicle. The idea behind the proposed method is that, when a vehicle passes a bridge, there would be a local peak in the time history of the specific low-pass filtered acceleration, which is essentially the dynamic responses induced by the driving force, of the bridge. Several matrix equations are used to establish a simple relationship between the characteristics of the low-pass filtered vehicle acceleration and the location of the damage.

The existence of the local peak is discussed and verified with a series of finite element analyses. Observations show that the proposed method can effectively identify the location of the damage.

Keywords: Damage localisation · Vehicle-bridge-interaction (VBI) system · Driving force · Drive-by Method

1 Introduction

Short and medium span bridges make up a large proportion of urban transport systems. With ageing structures and increasing transport demand, the number of bridges in need of maintenance has increased rapidly in recent years. In the UK, the cost is estimated to be £5 billion between 2019 and 2020 [1]. Therefore, early detection of bridge damage is a necessary and effective process to ensure the safety of transport systems [2] and reduce maintenance costs. Some scientists have participated in the use of a moving instrumented vehicle, the drive-by method, to identify the frequency of bridges to check

M. P. Limongelli et al. (Eds.): EVACES 2023, LNCE 433, pp. 155–164, 2023.
https://doi.org/10.1007/978-3-031-39117-0_16

their health status [3–5]. Compared with the traditional method of installing sensors on bridges, which requires a lot of labour, time and equipment costs, the drive-by method should be more effective and economical. However, it is still a problem to locate damage with moving vehicles.

To solve this problem, the key issue is to find the relationship between the damage location and the bridge responses. Scientists have proposed many methods to analyse damage induced changes in structural properties (stiffness, modal damping and mode shapes) and then locate structural damage. A typical method is to use model updating [6], which turns out to be time-consuming, to explore potentially damaged sections on a bridge by changing the model properties. The landmark research was the proposal of Zhu and Law in 2005 [7]. They used the continuous wavelet transform to analyse the operational deflection time history in the mid-span of a bridge subjected to a moving vehicle load. Instead of directly examining the change in material properties, continuity of functions or eigen functions of the influence line, mode shape and mode shape curvature are used to perform damage localisation in time. Potentially damaged sections can be found by searching for singularities on corresponding function curves. This type of singularity has then been used in subsequent research with various methods: Roveri and Carcaterra [8] used the Hilber-Huang transform (HHT), Khorram et al. [9] used wavelet analysis combined with factorial design, and Zhang et al. [10] used an instantaneous amplitude squared (IAS) combined Hilbert transform to check the singularities of corresponding bridge or vehicle responses. Nie et al. [11] located damage by searching for singularities in the cross-correlation function between two sensors in a moving mass model. Compared to model updating, the landmark research does not require a finite element model and is therefore more efficient.

A shortcoming of Zhu and Law's research is that the relationship between damage location and bridge response was proposed based on a rotational spring model. Damaged sections were assumed to be rotational springs, which is different from the realistic condition. He and Zhu [12] used a more realistic model with a local stiffness reduced region instead of the rotational springs. However, [12] focuses on the dynamic vertical displacement of the bridge, which is difficult to measure accurately in engineering. Furthermore, although they [12] derived an analytical solution from the partial differential dynamic equations of a damaged beam under a moving force, the solution is very complex and involves many solvable but implicit parameters. Therefore, it would be rather difficult to establish a direct theoretical relationship between structural damage and structural response. In their study [12], some damage indices are derived from finite element simulations rather than from the derived analytical solution. In addition, they focus on the high frequency bridge frequency related (BFR [13]) bridge vibration component.

In this study, we have proposed a new method for the location of structural damage using the directly measured acceleration of the vehicle. In order to develop this method, a theoretical derivation was proposed to provide a straightforward explanation of the relationship between damage location and driving force related (DFR [13]) bridge responses. Accordingly, a drive-by method was proposed for damage localisation of short and medium span bridges from low-pass filtered vehicle acceleration. In Sect. 3, two finite element models were constructed to validate the theoretical derivations.

2 Theoretical Derivation of Dynamic Responses of VBI Systems

2.1 Dynamic Responses of a Health Beam Under a Moving Vehicle

The dynamic equations of a simple VBI system (shown in Fig. 1) were listed as follows (Eq. (1) and Eq. (2)). The vehicle is simplified as a single-degree-of-freedom system consisting of a spring and a sprung mass.

$$m_v\ddot{u}_v(t) + k_v[u_v(t) - u_w(t)] = 0 \tag{1}$$

$$\overline{m}\ddot{u}_b(x,t) + EIu_b''''(x,t) = \{k_v\left[u_v(t) - u_b(x,t)|_{x=vt}\right] - m_vg\}\delta(x - vt) \tag{2}$$

where $\overline{m}$ is the unit mass, E is the elastic modulus, I is the moment of inertia. g is the acceleration of gravity, and a prime denotes differentiation to coordinate x of the beam.

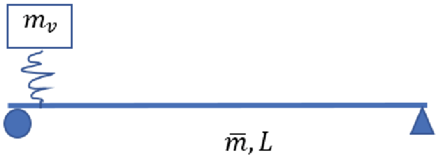

Fig. 1. Single degree of freedom (SDOF) VBI system.

As derived in [14], when the mass of the vehicle is much smaller than that of the bridge, the solution of Eq. (2) is,

$$u_b(x,t) = \sum\nolimits_n \frac{\Delta_{st,n}}{1 - S_n^2}\{sin\frac{n\pi x}{L}[sin\frac{n\pi vt}{L} - S_n sin\omega_{b,n}t]\} \tag{3. a}$$

where

$$\Delta_{st,n} = \frac{-2m_vgL^3}{n^4\pi^4EI} \tag{3. b}$$

$$S_n = \frac{n\pi v}{L\omega_{b,n}} \tag{3. c}$$

$$\omega_{b,n} = \frac{n^2\pi^2}{L^2}\sqrt{\frac{EI}{\overline{m}}} \tag{3. d}$$

It should be noted that the $u_b(x,t)$ is essentially a dynamic bridge response under a constant moving force m_vg. Equation (3. a) can be furtherly separated as two components:

$$u_{b,DFR}(x,t) = \sum\nolimits_n \frac{\Delta_{st,n}}{1 - S_n^2} sin\frac{n\pi x}{L} sin\frac{n\pi vt}{L} \tag{4}$$

$$u_{b,BFR}(x,t) = \sum\nolimits_n \frac{\Delta_{st,n}}{1 - S_n^2}(-S_n sin\omega_{b,n}t) \tag{5}$$

Equation (4) is the DFR components corresponding to the driving-force frequencies,

$$\Omega_n = \frac{n\pi v}{l} \tag{6}$$

while Eq. (5) denotes the BFR components corresponding to bridge natural frequencies $\omega_{b,n}$. As reported by He and Zhu in their research [13], the ratio between Ω_1 and $\omega_{b,1}$ is always less than 0.15. Also, in this study, the moving speed is set to be much slower than the general moving speeds, which makes the approximation ([15], Eq. (7)) is acceptable,

$$\begin{aligned} u_{b,DFR}(x,t) &= y_{static}(x, a|_{a=vt}) \\ &= \begin{cases} \frac{m_v g}{EI_0}\left(\frac{x}{6l}a^3 - \frac{x}{2}a^2 + \frac{2(xl^2+x^3)}{6l}a - \frac{x^3}{6l}\right) & (a > x) \\ \frac{m_v g}{EI_0}\left(\frac{(x-l)}{6l}a^3 + \frac{x^3-3lx^2+2l^2x}{6l}a\right) & (a < x) \end{cases} \end{aligned} \tag{7}$$

Equation (7) denotes that the DFR deflection is approximately equal to the static deflection under the constant force $m_v g$. Then the following matrix equation can be derived,

$$[\mathrm{K}]\left\{u_{b,DFR}\right\}^t = \{m_v g\}^t \tag{8. a}$$

where [K] is the stiffness matrix of the beam. Moreover, since the $u_{b,BFR}(x,t)$ is a kind of free vibration, the following equation can be derived,

$$[\mathrm{M}]\left\{\ddot{u}_{b,DFR}\right\}^t + [\mathrm{K}]\left\{u_{b,DFR}\right\}^t = \{m_v g\}^t \tag{8. b}$$

Equation (7) indicates that the $u_{b,DFR}(x,t)$ is a piecewise cubic function. Therefore the $\left\{\ddot{u}_{b,DFR}\right\}^t$, which equals twice the differentiation of $\left\{u_{b,DFR}\right\}^t$, should be a piecewise linear function whose turning point is the time point when the moving vehicle is right on the observation point.

2.2 Dynamic Responses of the Vehicle in a Health VBI System

One can get the DFR deflection of the contact point by changing the x into $a|_{a=vt}$ in Eq. (7). Then it can be derived that the low-pass filtered trajectory of the contact point, i.e., the low-frequency components of $u_w(t)$ which can be achieved with an integral process of the $u_{b,DFR}(x,t)$, is a continuous quartic function. As a foundation motion in the vertical direction, it can be derived from Eq. (1) that the low-pass filtered displacement of the vehicle should be a quartic function. Furthermore, for a health bridge, the low-passed filtered acceleration of the vehicle in the vertical direction should be a quadratic function.

2.3 Dynamic Responses of a Damaged Beam in a VBI System

In this study, bridge damage is modeled as stiffness reduction in a local section. While the mass of a damaged beam keeps unchanged. As shown in Fig. 2, the damaged region ranges from the coordinated x_1 to x_2. We assume that the stiffness of the beam in the

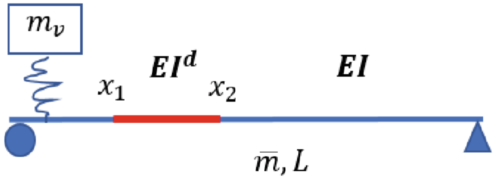

Fig. 2. Single degree of freedom (SDOF) VBI system. (x_1 to x_2 is the damaged region)

damaged section reduces from EI to EI^d. It is also assumed that the mass of the vehicle is much smaller than the bridge. Similarly, as dynamic bridge responses derived in Eq. (3. a), the dynamic responses of the bridge can be approximately calculated through a driving-force model. Then the dynamic matrix equation of the damaged beam is,

$$[\mathrm{M}]\left\{\ddot{u}_b^d\right\}^t + [\mathrm{K}^d]\left\{u_b^d\right\}^t = \{m_v g\}^t \tag{9}$$

The [M] is the mass matrix which assumes to be the same between the damaged beam and the corresponding health beam. $[\mathrm{K}^d]$ is the stiffness matrix of the damaged beam. $\left\{\ddot{u}_b^d\right\}^t$ is the vector of the acceleration of beam nodes at the time point t. $\left\{u_b^d\right\}^t$ is the vector of deflection of beam nodes at t. To check the influence of bridge damage on the difference of bridge dynamics between a health and a damage beam, we define that,

$$\left\{\ddot{u}_b^d\right\}^t = \{\ddot{u}_b\}^t + \left\{\ddot{u}_b^\Delta\right\}^t \tag{10. a}$$

$$\left\{u_b^d\right\}^t = \left\{u_b\right\}^t + \left\{u_b^\Delta\right\}^t \tag{10. b}$$

$$\left[\mathrm{K}^d\right] = [\mathrm{K}] + [\mathrm{K}^\Delta] \tag{10. c}$$

where the superscript Δ denotes the difference in corresponding parameters or responses between healthy and damaged beams. Then Eq. (9) can be expanded as Eq. (11).

$$[\mathrm{M}](\{\ddot{u}_b\}^t + \left\{\ddot{u}_b^\Delta\right\}^t) + ([\mathrm{K}] + [\mathrm{K}^\Delta])(\left\{u_b\right\}^t + \left\{u_b^\Delta\right\}^t) = \{m_v g\}^t \tag{11}$$

Further, Eq. (11) and be divided into two sub-equations,

$$[\mathrm{M}]\left\{\ddot{u}_b\right\}^t + [\mathrm{K}]\left\{u_b\right\}^t = \{m_v g\}^t \tag{12. a}$$

$$[\mathrm{M}]\left\{\ddot{u}_b^\Delta\right\}^t + [\mathrm{K}]\left\{u_b^\Delta\right\}^t + \left[\mathrm{K}^\Delta\right]\left\{u_b^\Delta\right\}^t = -[\mathrm{K}^\Delta]\left\{u_b\right\}^t \tag{12. b}$$

It should be noted that $\{\ddot{u}_b\}^t$ and $\left\{u_b\right\}^t$ are the dynamic responses of the healthy beam, therefore Eq. (12. a) would always holds. While for Eq. (12. b), in this study, the term $\left[\mathrm{K}^\Delta\right]\left\{u_b^\Delta\right\}^t$ is supposed to be neglectable, and Eq. (12. b) would be simplified as,

$$[\mathrm{M}]\left\{\ddot{u}_b^\Delta\right\}^t + [\mathrm{K}]\left\{u_b^\Delta\right\}^t = -[\mathrm{K}^\Delta]\left\{u_b\right\}^t \tag{13}$$

Similarly as the separation illustrated in Eq. (4) and Eq. (5), the $\{u_b\}^t$ can be separated as a summation of two vectors (shown as Eq. (14)),

$$\{u_b\}^t = \{u_{b,DFR}\}^t + \{u_{b,BFR}\}^t \tag{14}$$

Then, Eq. (13) is correspondingly separated into two sub-equations,

$$[\mathrm{M}]\{\ddot{u}^{\Delta}_{b,DFR}\}^t + [\mathrm{K}]\{u^{\Delta}_{b,DFR}\}^t = -[\mathrm{K}^{\Delta}]\{u_{b,DFR}\}^t \tag{15. a}$$

$$[\mathrm{M}]\{\ddot{u}^{\Delta}_{b,BFR}\}^t + [\mathrm{K}]\{u^{\Delta}_{b,BFR}\}^t = -[\mathrm{K}^{\Delta}]\{u_{b,BFR}\}^t \tag{15. b}$$

In this study, we mainly focuses on the low-frequency vibration components, i.e., the Eq. (15. a). Since Eq. (8. a) indicates that

$$\{u_{b,DFR}\}^t = [\mathrm{K}]^{-1}\{m_v g\}^t \tag{16}$$

where $[\mathrm{K}]^{-1}$ is the inverse matrix of [K], one can contain Eq. (17) by substituting Eq. (16) into Eq. (15. a),

$$[\mathrm{M}]\{\ddot{u}^{\Delta}_{b,DFR}\}^t + [\mathrm{K}]\{u^{\Delta}_{b,DFR}\}^t = -[\mathrm{K}^{\Delta}][\mathrm{K}]^{-1}\{m_v g\}^t \tag{17}$$

As for the "damage factor", i.e., the matrix product of $[\mathrm{K}^{\Delta}][\mathrm{K}]^{-1}$, assume that the number of the node in x_1 is i, and the node number at x_2 is j, then $[\mathrm{K}^{\Delta}][\mathrm{K}]^{-1}$ would be

$$[\mathrm{K}^{\Delta}][\mathrm{K}]^{-1} = \left[\begin{array}{ccccccccccccccc}
\cdots & \cdots & (i-1)_2 & i_1 & i_2 & (i+1)_1 & (i+1)_2 & (i+2)_1 & (i+2)_2 & \cdots & (j-1)_2 & j_1 & j_2 & (j+1)_1 \\
\cdots & \cdots & \ddots & \vdots & \vdots & \vdots & \vdots & \vdots & \vdots & \vdots & \vdots & \vdots & \vdots & \vdots \\
(i-1)_2 & \vdots & 0 & 0 & 0 & 0 & 0 & 0 & 0 & \cdots & 0 & 0 & 0 & 0 \\
i_1 & \vdots & X_{i_1,(i-1)_2} & X_{i_1,i_1} & X_{i_1,i_2} & X_{i_1,(i+1)_1} & X_{i_1,(i+1)_2} & X_{i_1,(i+2)_1} & X_{i_1,(i+2)_2} & \cdots & X_{i_1,(j-1)_2} & X_{i_1,j_1} & X_{i_1,j_2} & X_{i_1,(j+1)_1} \\
i_2 & \vdots & Y_{i_2,(i-1)_2} & Y_{i_2,i_1} & Y_{i_2,i_2} & Y_{i_2,(i+1)_1} & Y_{i_2,(i+1)_2} & Y_{i_2,(i+2)_1} & Y_{i_2,(i+2)_2} & \cdots & Y_{i_2,(j-1)_2} & Y_{i_2,j_1} & Y_{i_2,j_2} & Y_{i_2,(j+1)_1} \\
(i+1)_1 & \vdots & 0 & 0 & 0 & \lambda & 0 & 0 & 0 & \cdots & 0 & 0 & 0 & 0 \\
(i+1)_2 & \vdots & 0 & 0 & 0 & 0 & \lambda & 0 & 0 & \cdots & 0 & 0 & 0 & 0 \\
(i+2)_1 & \vdots & 0 & 0 & 0 & 0 & 0 & \lambda & 0 & \cdots & 0 & 0 & 0 & 0 \\
(i+2)_2 & \vdots & 0 & 0 & 0 & 0 & 0 & 0 & \lambda & \cdots & 0 & 0 & 0 & 0 \\
\vdots & \vdots & \vdots & \vdots & \vdots & \vdots & \vdots & \vdots & \vdots & \vdots & \vdots & \vdots & \vdots & \vdots \\
(j-1)_2 & \vdots & 0 & 0 & 0 & 0 & 0 & 0 & 0 & \cdots & \lambda & 0 & 0 & 0 \\
j_1 & \vdots & V_{j_1,(i-1)_2} & V_{j_1,i_1} & V_{j_1,i_2} & V_{j_1,(i+1)_1} & V_{j_1,(i+1)_2} & V_{j_1,(i+2)_1} & V_{j_1,(i+2)_2} & \cdots & V_{j_1,(j-1)_2} & V_{j_1,j_1} & V_{j_1,j_2} & V_{j_1,(j+1)_1} \\
j_2 & \vdots & W_{j_2,(i-1)_2} & W_{j_2,i_1} & W_{j_2,i_2} & W_{j_2,(i+1)_1} & W_{j_2,(i+1)_2} & W_{j_2,(i+2)_1} & W_{j_2,(i+2)_2} & \cdots & W_{j_2,(j-1)_2} & W_{j_2,j_1} & W_{j_2,j_2} & W_{j_2,(j+1)_1} \\
(j+1)_1 & \vdots & 0 & 0 & 0 & 0 & 0 & 0 & 0 & 0 & 0 & 0 & 0 & 0 \\
\vdots & \vdots & \vdots & \vdots & \vdots & \vdots & \vdots & \vdots & \vdots & \vdots & \vdots & \vdots & \vdots & \vdots
\end{array}\right] \tag{18}$$

where X, Y, and λ are constant parameters related with the EI^d. It can be concluded from Eq. (18) that when the vehicle arrives at a damaged section, the product of $[\mathrm{K}^{\Delta}][\mathrm{K}]^{-1}$ and $\{m_v g\}^t$ is a constant non-zero external force. While before or after the vehicle locates in the damaged section, the product of $[\mathrm{K}^{\Delta}][\mathrm{K}]^{-1}$ and $\{m_v g\}^t$ the force would become zero (as illustrated in Fig. 3).

Similarly, as the transformation from Eq. (8. b) to Eq. (8. a), it is supposed that $\{u^{\Delta}_{b,DFR}\}^t$ can be approximately calculated from Eq. (17) to Eq. (19),

$$[\mathrm{K}]\{u^{\Delta}_{b,DFR}\}^t = -[\mathrm{K}^{\Delta}][\mathrm{K}]^{-1}\{m_v g\}^t \tag{19}$$

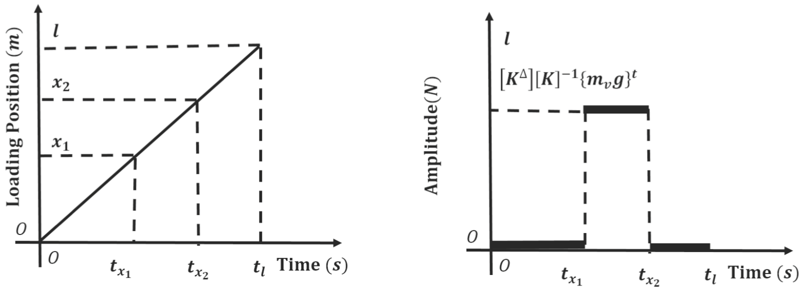

(a) Loading position (b) Magnitude*

Fig. 3. Loading position and amplitude of $[K^{\Delta}][K]^{-1}\{m_v g\}^t$ (*t_{x_1}, t_{x_2} are the time points when the vehicle moves at x_1, x_2, respectively.)

Equation (19) is essentially a static equation. Since $[K^{\Delta}][K]^{-1}\{m_v g\}^t$ equals $\lambda m_v g$, which is a constant moving force, it can be derived that when the vehicle arrives in the damaged section, the $\lambda m_v g$ would induce a extra low-pass filtered bridge deflation. As derived in Eq. (7), time history of the extra deflection should be a piece of cubic function. Correspondingly, the extra low-pass filtered bridge acceleration should be a piece of linear function which might appear as a "bump".

2.4 Low-Pass Filtered Responses of the Vehicle Running on a Damaged Bridge

Similarly, following the same derivation process in Sect. 2.2, the extra bridge deflection induced by $\lambda m_v g$ would induce an extra vertical displacement of the contact point when the vehicle moves onto the damaged region, which should a piece of a quartic function. Furtherly, there should be a extra piece of quadratic function in the low-pass filtered vehicle acceleration. Therefore, the structural damage can be directly located by searching for the "bump" on the low-pass filtered vehicle acceleration.

3 Validation with Finite Element Models

To validate the proposed damage localisation method, a health VBI system model and a corresponding model with a damaged beam were built with the finite element method. The health VBI system model consists of a simply supported beam and a simplified quarter car model. The bridge span length is 20 m. The cross-section is constant. The moment of inertia is 0.001067 m^4, Young's modulus is 210 GPa, and the mass per unit length is 7850 kg/m. The sprung mass is 2,415 kg. The spring stiffness is 157, 754 N/m. The vehicle moves with a constant speed of 0.9 m/s from 0.2 m to 18.2 m. The sampling period is set as 0.01 s. As for the structural damage, the stiffness of the damaged section (from 12.5 m to 15 m) is half of that of health sections.

The simulation was proposed with ABAQUS [16]. The simulation method has been introduced and verified in the previous research [17]. The observation point is 0.5 m ahead of the damaged region. The cutting frequency was selected as 0.1 Hz, which is higher than the Ω_1 and is much lower than the bridge first natural frequency.

Figure 4 a. illustrates the low-pass filtered [18] acceleration of the health beam under the moving vehicle. The time point when the vehicle moves right on the observation point (at 13.33 s) is marked with a red circle. Time history of this acceleration is a piecewise linear function of which the turning point is the time point when the vehicle is moving upon the selected observation point, which coincides with the derived theoretical derivation in Sect. 2. While for the time history of the low-pass filtered vehicle acceleration (shown in Fig. 4 b.), although the acceleration curve also includes some high-frequency components, the baseline presents with a continuous function shape. Figure 4 c. illustrates the low-pass filtered acceleration of a damaged beam under the same moving vehicle. The vehicle enters the damaged region at 13.89 s, and leaves the damaged region at 16.66 s. Both of the enter and the exit time points are marked with dash lines, respectively. A obvious "bump" can be found in the corresponding damaged section, which coincides with the theoretical derivation. Figure 4 d. illustrates the acceleration time history of the low-pass filtered vehicle acceleration when the vehicle moves on the damaged beam, another "bump" can be found on the corresponding time point when the vehicle locates above the damaged section, which validates the effectiveness of the proposed method for damage localisation.

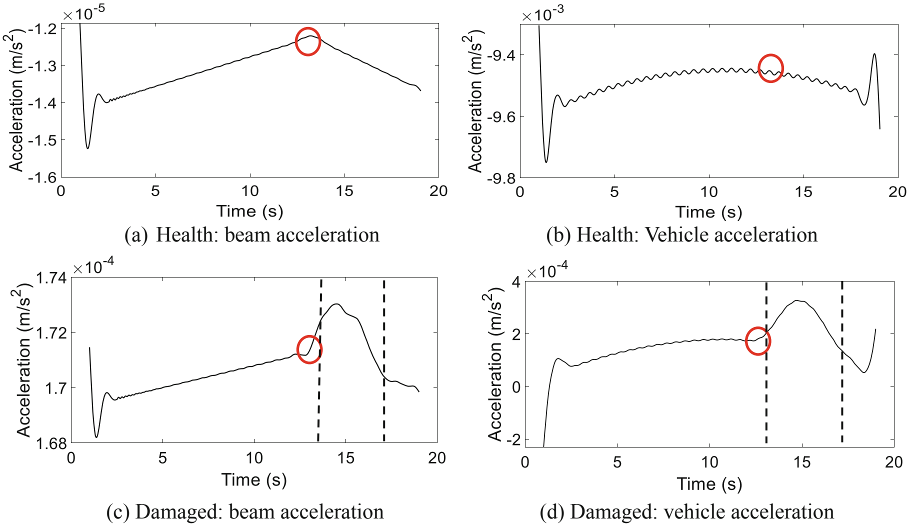

(a) Health: beam acceleration

(b) Health: Vehicle acceleration

(c) Damaged: beam acceleration

(d) Damaged: vehicle acceleration

Fig. 4. Simulation results of VBI system models

(Red circle: The vehicle moves right on the observation point at 13.33 s. Dashed lines: The vehicle enters the damaged region at 13.89 s, and leaves the damaged region at 16.66 s.)

4 Conclusions

In this study, a novel drive-by damage localisation method was proposed based on the theoretical derivation for a simple relationship between the low-frequency bridge vibration and the damage location. The structural damage was transformed into an external force applied to a healthy beam. It should then be possible to use an instrumented vehicle to locate the damage by searching for the "bump" on the low-pass filtered time history of the vehicle acceleration. The main conclusions are as follows,

(1) For a healthy beam, the low frequency bridge deflection is approximately equal to the static deflection under a moving vehicle gravity at low travelling speeds.
(2) For a damaged beam, the structural damage acts as a time-varying external force applied to the beam. If the vehicle is moving towards the damaged section, this external force shall be non-zero; otherwise it shall be zero.
(3) For a damaged beam, "bump" would occur at the time points of both the low-pass filtered bridge acceleration and vehicle acceleration time histories when the moving vehicle is directly on the damaged section, which can be used to locate potential damage.

The availability of the proposed method would be investigated in the further study with laboratory experiments and field tests.

References

1. Huseynov, F., Kim, C., OBrien, E.J., Brownjohn, J.M.W., Hester, D., Chang, K.C.: Bridge damage detection using rotation measurements – experimental validation. Mech. Syst. Signal Process. **135**, 106380 (2020)
2. Krieger, J.: European Bridge maintenance: Monitoring safety in Germany (2019). https://www.governmenteuropa.eu/european-bridge-maintenance/92201/
3. Yang, Y.B., Xu, H., Mo, X.Q., Wang, Z.L., Wu, Y.T.: An effective procedure for extracting the first few bridge frequencies from a test vehicle. Acta Mech. **232**(3), 1227–1251 (2021). https://doi.org/10.1007/s00707-020-02870-w
4. Yang, Y.B., Lin, C.W., Yau, J.D.: Extracting bridge frequencies from the dynamic response of a passing vehicle. J. Sound Vib. **272**(3–5), 471–493 (2004)
5. Siringoringo, D.M., Fujino, Y.: Estimating bridge fundamental frequency from vibration response of instrumented passing vehicle: analytical and experimental study. Adv. Struct. Eng. **15**(3), 417–433 (2012)
6. Abedin, M., De Caso y Basalo, F.J., Kiani, N., Mehrabi, A.B., Nanni, A.: Bridge load testing and damage evaluation using model updating method. Eng. Struct. **252**, 113648 (2022)
7. Zhu, X.Q., Law, S.S.: Wavelet-based crack identification of bridge beam from operational deflection time history. Int. J. Solids Struct. **43**, 2299–2317 (2006)
8. Roveri, N., Carcaterra, A.: Damage detection in structures under traveling loads by Hilbert-Huang transform. Mech. Syst. Signal Process. **28**, 128–144 (2012)
9. Khorram, A., Bakhtiari-Nejad, F., Rezaeian, M.: Comparison studies between two wavelet based crack detection methods of a beam subjected to a moving load. Int. J. Eng. Sci. **51**, 204–215 (2012)
10. Zhang, B., Qian, Y., Wu, Y., Yang, Y.B.: An effective means for damage detection of bridges using the contact-point response of a moving test vehicle. J. Sound Vib. **419**, 158–172 (2018)

11. Nie, Z., Lin, J., Li, J., Hao, H., Ma, H.: Bridge condition monitoring under moving loads using two sensor measurements. Struct. Health Monit. **19**, 917–937 (2020)
12. He, W.-Y., Zhu, S.: Moving load-induced response of damaged beam and its application in damage localisation. J. Vib. Control **22**, 3601–3617 (2022)
13. Yang, Y.B., Lin, C.W.: Vehicle–bridge interaction dynamics and potential applications. J. Sound Vib. **284**, 205–226 (2005)
14. Yang, Y.B., Chang, K.C.: Extracting the bridge frequencies indirectly from a passing vehicle: parametric study. Eng. Struct. **31**, 2448–2459 (2009)
15. Frýba, L.: Vibration of Solids and Structures Under Moving Loads. Springer, Heidelberg (2013). https://doi.org/10.1007/978-94-011-9685-7
16. Smith, M.: ABAQUS/Standard User's Manual, Version 6.9. Dassault Systèmes Simulia Corp. (2009)
17. Lu, X., Kim, C.-W., Chang, K.-C.: Finite element analysis framework for dynamic vehicle-bridge interaction system based on ABAQUS. Int. J. Struct. Stab. Dyn. **20**, 2050034 (2020)
18. Mathworks Inc. (2021)